Supplementary Materials: Experimental Realization of an Intrinsic Magnetic Topological Insulator

Yan Gong (龚演)[1], Jingwen Guo (郭景文)[1], Jiaheng Li (李佳恒)[1], Kejing Zhu (朱科静)[1], Menghan Liao (廖孟涵)[1], Xiaozhi Liu (刘效治)[2], Qinghua Zhang (张庆华)[2], Lin Gu (谷林)[2], Lin Tang (唐林)[1], Xiao Feng (冯硝)[1], Ding Zhang (张定)[1,3,4], Wei Li (李渭)[1,4], Canli Song (宋灿立)[1,4], Lili Wang (王立莉)[1,4], Pu Yu (于浦)[1,4], Xi Chen (陈曦)[1,4], Yayu Wang (王亚愚)[1,3,4], Hong Yao (姚宏)[4,5], Wenhui Duan (段文晖)[1,3,4], Yong Xu (徐勇)[1,4,6*], Shou-Cheng Zhang (张首晟)[7], Xucun Ma (马旭村)[1,4], Qi-Kun Xue (薛其坤)[1,3,4*], Ke He (何珂)[1,3,4*]

[1]*State Key Laboratory of Low Dimensional Quantum Physics, Department of Physics, Tsinghua University, Beijing 100084*

[2]*Beijing National Laboratory for Condensed Matter Physics, Institute of Physics, Chinese Academy of Sciences, Beijing 100190*

[3]*Beijing Academy of Quantum Information Sciences, Beijing 100193*

[4]*Collaborative Innovation Center of Quantum Matter, Beijing 100084*

[5]*Institute for Advanced Study, Tsinghua University, Beijing 100084*

[6]*RIKEN Center for Emergent Matter Science (CEMS), Wako, Saitama 351-0198, Japan*

[7]*Stanford Center for Topological Quantum Physics, Department of Physics, Stanford University, Stanford, California 94305-4045, USA*

**Correspondence authors. Email: yongxu@mail.tsinghua.edu.cn; qkxue@mail.tsinghua.edu.cn; kehe@tsinghua.edu.cn

Methods

Molecular beam epitaxy (MBE) growth of $MnBi_2Te_4$ films and angle-resolved photoemission spectroscopy (ARPES) measurements were carried out in one ultrahigh vacuum (UHV) system with a base pressure 1×10^{-10} mbar. Si(111) substrates were cleaned by repeated rapid heating (flashing) up to 1100℃ until they show clean 7×7 surface reconstruction. $SiTiO_3$(111) substrates were processed by annealing in oxygen up to 930℃ before they were loaded to the UHV chamber and outgassed at 400℃ for half an hour. High purity Bi (99.999%), Te (99.9999%) and Mn (99.999%) were evaporated with standard Knudsen cells. Bi_2Te_3 films were grown on Si (111) or $SrTiO_3$(111) substrates that were kept at 200℃. Then Mn and Te were co-deposited on Bi_2Te_3 at 200℃ with post-annealing at the same temperature for 10 min, which leads to formation of $MnBi_2Te_4$. ARPES measurements were carried out with unpolarized He-Iα photons (21.21 eV) generated by a Gammadata He discharge lamp and a Scienta-R4000 analyzer. The samples were cooled with liquid He-4 to ~ 25 K in measurements. The samples for SQUID and Hall measurements

were capped by a Te layer of ~ 20 nm before loaded out of the UHV chamber.

SQUID measurements were performed in a commercial MPMS-52 system (Quantum Design). The linear diamagnetic backgrounds of the substrates and capping layers were subtracted from all data.

Transport measurements were carried out in a closed cycle system (Oxford Instruments TelatronPT) (base temperature=1.5 K). Freshly cut indium cubes were cold pressed onto the sample as contacts. Standard lock-in techniques were employed to determine the sample resistance in a four-terminal configuration with a typical excitation current of 100 nA at 13 Hz.

First-principles density functional theory calculations were performed using the projector augmented wave method [1,2] and the plane-wave basis with an energy cutoff of 350 eV, as implemented in the Vienna *ab initio* simulation package [3]. The Perdew-Burke-Ernzerhof type exchange correlation functional [4] in the generalized gradient approximation (GGA) was employed together with the GGA+*U* method [5] to treat the localized 3*d* orbitals of Mn (U = 4 eV). The Monkhorst-Pack **k**-grids of $12 \times 12 \times 1$ and $9 \times 9 \times 3$ were selected for calculations of thin films and bulk $MnBi_2Te_4$, respectively. Structure optimizations were carried out with a force convergence criterion of 0.01eV/Å. Van der Waals corrections [6] were included to describe interlayer interactions in multi-layer and bulk $MnBi_2Te_4$.

Reflection high energy electron diffraction (RHEED)

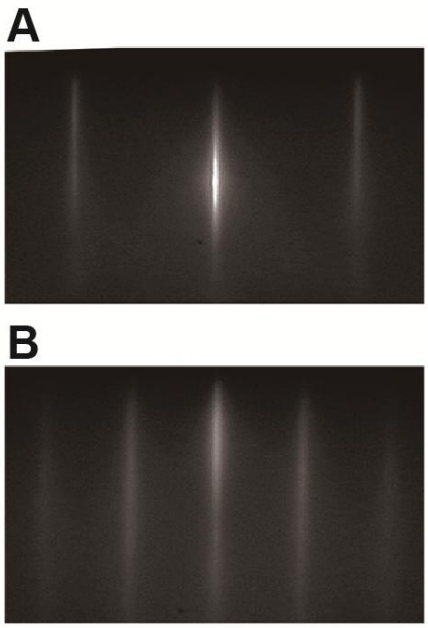

Fig. S1. RHEED patterns of $MnBi_2Te_4$ along [112] and [110] directions, respectively. The sharp diffraction steaks indicate the two-dimensional morphology and high quality of the film.

Raw SQUID data

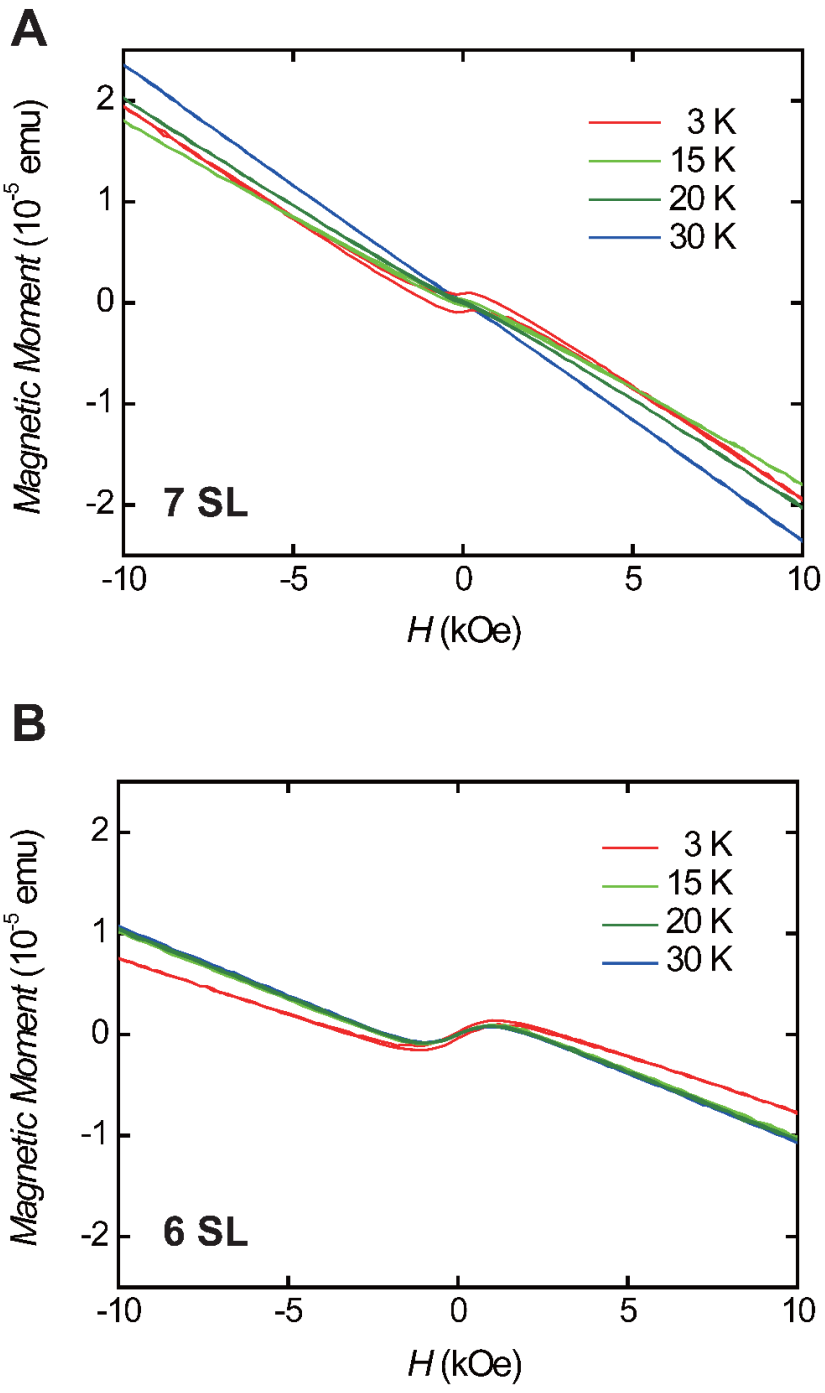

Fig. S2. Raw SQUID data of the 7 SL (A) and 6 SL (B) $MnBi_2Te_4$ film at different temperatures. Subtracting linear diamagnetic backgrounds from these data, we obtain the data shown in Figs. 3(a) and 3(b).

Theoretical study of magnetic ground states

Firstly, different spin configurations in monolayer $MnBi_2Te_4$ were considered, including FM, stripy AFM, zigzag AFM and in-plane AFM (Fig. S3). Their total energies (referenced to the FM state) are 0.0, 5.0, 5.4 and 6.4 meV, respectively. The calculated exchange interactions between the nearest-neighbor (J_1) and next nearest-neighbor spins (J_2) are J_1 = -1.4 meV and J_2 = 0.2 meV. These data suggest that the exchange coupling is ferromagnetic within the monolayer. Secondly, the out-of-plane ferromagnetism in monolayer $MnBi_2Te_4$ gives a total energy 0.25 meV/unit lower than the in-plane ferromagnetism, implying an out-of-plane easy axis. Thirdly, the *A*-type AFM bulk gives a total energy per formula unit 1.2meV lower than the FM bulk, which is the magnetic ground state of $MnBi_2Te_4$.

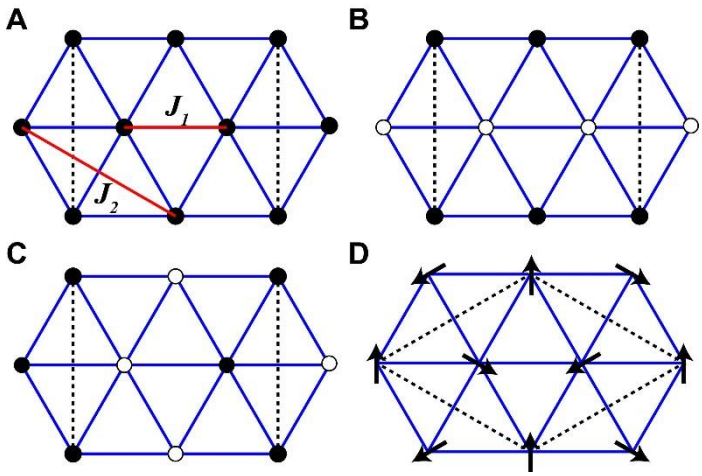

Fig. S3. Top view of different spin configurations of Mn atoms in monolayer $MnBi_2Te_4$: (**A**) FM, (**B**) stripy AFM, (**C**) zigzag AFM, and (**D**) in-plane AFM. Mn atoms form a triangular lattice. Supercell cells are denoted by dashed lines. Up, down and in-plane spins are denoted by black filled circles, open circles and arrows, respectively. Exchange interaction between the nearest-neighbor (J_1) and next nearest-neighbor spins (J_2) are denoted by red lines.

Band structures of $MnBi_2Te_4$ thin films

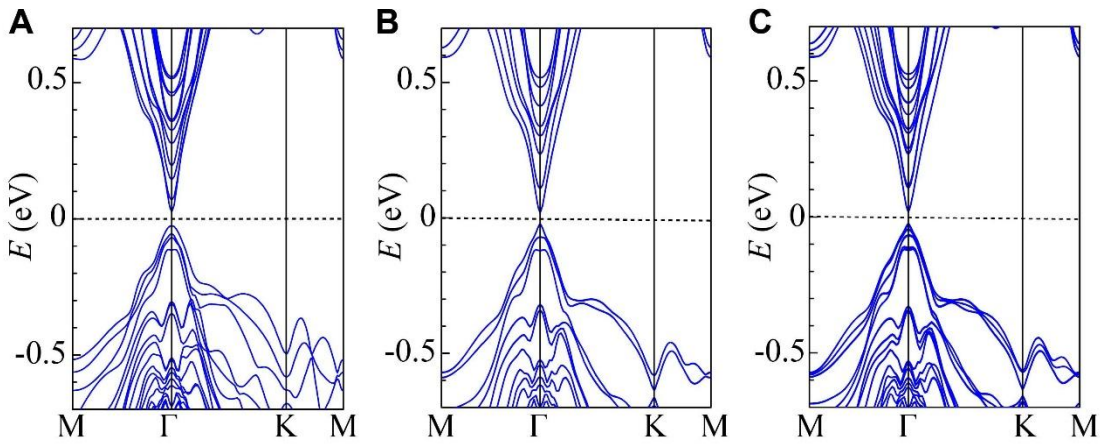

Fig. S4. (**A**)-(**C**) Band structures of $MnBi_2Te_4$ thin films with a thickness of (**A**) 3, (**B**) 4 and (**C**) 6 SLs. Their calculated band gaps are 50, 40 and 51 meV, respectively.

References

[1] P. E. Blöchl, Phys. Rev. B **50**, 17953 (1994).
[2] G. Kresse, D. Joubert, Phys. Rev. B **59**, 1758 (1999).
[3] G. Kresse, J. Furthmuller, Phys. Rev. B **54**, 11169 (1996).
[4] J. P. Perdew, K. Burke, M. Ernzerhof, Phys. Rev. Lett. **77**, 3865 (1996).
[5] S. Dudarev, G. Botton, S. Savrasov, C. Humphreys, A. Sutton, Phys. Rev. B **57**, 1505 (1998).
[6] S. Grimme, J. Antony, S. Ehrlich, and S. Krieg, J. Chem. Phys. **132**, 154104 (2010).